On lyotropic behavior of molecular bottle-brushes

Saariaho, M.; Ikkala, O.; Szleifer, I.; Erukhimovich, I.; ten Brinke, G.

Published in:
Journal of Chemical Physics

DOI:
10.1063/1.474677

On lyotropic behavior of molecular bottle-brushes: A Monte Carlo computer simulation study

Mika Saariaho and Olli Ikkala
Department of Engineering Physics and Mathematics, Helsinki University of Technology, P.O. Box 2200, FIN-02015 HUT Espoo, Finland

Igal Szleifer
Department of Chemistry, Purdue University, West-Lafayette, Indiana 47907

Igor Erukhimovich
Department of Physics, Moscow State University, Moscow 117234, Russia

Gerrit ten Brinke[a)]
Department of Polymer Science, Materials Science Center, University of Groningen, Nijenborgh 4, 9747 AG Groningen, The Netherlands

(Received 8 November 1996; accepted 8 May 1997)

A three dimensional continuous space Monte Carlo computer simulation study is presented to discuss the extension of flexible, linear polymer chains due to the presence of equally flexible side chains. We consider the enhancement of the persistence length of bottle-brush structures in an athermal solution due to steric interactions between the side chains. The largest structure studied consists of a backbone of 100 beads with 50 side chains of 20 beads each. The persistence length λ is evaluated in two different ways using the radius of gyration of the backbone and the bond angle correlation function, respectively. A correct description of the backbone conformations is shown to require at least two characteristic lengths. At a small length scale the backbone behaves flexible; the extension occurs at a larger length scale. There is a strong indication that the ratio between the persistence length and the diameter, which is the determining factor for lyotropic behavior of conventional semiflexible chains, levels off as a function of the side chain length. The value of this ratio is, moreover, too small to induce lyotropic behavior along this line. Recent experimental observations of lyotropic behavior of polymacromonomers are discussed in terms of these findings.
 [S0021-9606(97)53130-8]

I. INTRODUCTION

In the field of polymers, the phrase molecular bottle-brush is reserved for comb copolymers with a high density of side chains. Recently, the interest in comb copolymers has increased considerably mainly due to the introduction of two entirely different ''synthetic'' approaches. One class of systems was obtained by Schmidt and co-workers[1,2] who succeeded in polymerizing macromonomers resulting in high molar mass polymethacrylate backbones with oligostyrene side chains of up to 50 styrene units. Another related but quite different set of systems was obtained by various groups in a much simpler way using strong physical association between end-functionalized oligomeric chains and homopolymers.[3–11] Compared to the former systems, the oligomeric side chains used so far are, however, considerably smaller.

The physical association involves hydrogen bonding or ionic interactions. The hydrogen bonding systems are characterized by a somewhat weaker repulsion between the associated side chains and the polymer backbone and, therefore often exhibit order–disorder transitions in the melt.[8,9,11] The unfavorable interactions between the polar and nonpolar groups of the polyelectrolyte complexes are in general large and the systems studied so far all exhibit a microphase separated ordered state.[3–7,12] No order–disorder transitions have been observed. The phase behavior of both systems resembles in many ways that of ordinary comb copolymers,[13–16] however, in particular for the more weakly associating systems also interesting differences are predicted due to the reversible nature of the side chain association.[17,18] The above phase behavior concerns pure polymer-oligomer systems without additional solvent. In one case of the polyelectrolyte complex of poly(4-vinyl pyridine)-dodecyl benzene sulfonic acid (P4VP-DBSA), a selectively good solvent for the alkyl side chains, xylene, was added. The long period of the microphase separated lamellar structure increased for up to 60 wt % xylene, attributed to swelling of primarily the nonpolar alkyl layer. For higher amounts the order disappeared as demonstrated by a vanishing birefringence.[12]

The influence of particularly those solvents, which can be classified as good solvents for the side chains, is of interest because recent theoretical predictions contradict each other concerning the induced extension to the bottle-brushes. In a decade old publication Birshtein and co-workers[19] argued that comblike copolymers in dilute solution under good solvent conditions show considerable stretching of the polymer backbone and the side chains due to the excluded volume effect. They concluded that the repulsion increases the

[a)]Also at: Department of Engineering Physics and Mathematics, Helsinki University of Technology, P.O. Box 2200, FIN-02015 HUT Espoo, Finland.

extension of the structures leading to a persistence length in size comparable to the dimensions of the side chains. Conventional lyotropic behavior of semiflexible chains requires the ratio between the persistence length, characterizing the stiffness, and the diameter of the chain to be large (>10).[20,21] If this criterion is applied to molecular bottle-brushes, the prediction of Birshtein and co-workers implies that lyotropic behavior should not be expected. More recently, Fredrickson[22] came to exactly the opposite conclusion that flexible nonconjugated polymers can be made to exhibit nematic order by the proper choice of surfactant. He predicts in particular that under appropriate conditions the relevant ratio between the persistence length and the diameter of the bottle-brush increases monotonously as a function of the side chain length.

Schmidt and co-workers[1,2] succeeded in polymerizing polymacromonomers consisting of oligostyrene side chains of up to 50 styrene units leading to bottle-brushes with a high molar mass polymethacrylate (PMA) backbone. From dynamic light scattering data and x-ray scattering on dilute solutions in toluene they concluded that the PMA main chain adopted an extremely extended conformation characterized by a persistence length of up to 1000 Å, surrounded by expanded but still flexible polystyrene side chains. For increasing concentrations of the polymacromonomer in toluene small angle x-ray scattering showed the presence of a scattering peak which suddenly becomes narrow and large at ~ 31.5 wt %.[1] They tentatively concluded that a nematic solution was obtained as a consequence of the extension of the main chain due to steric interactions between the oligostyrene side chains. If this conclusion is correct it means that lyotropic behavior of bottle-brushes due to excluded volume interactions can be realized.

Molecular bottle-brushes obtained by physical association, notably hydrogen bonding, exhibit related behavior. In this case the explanation is rather straightforward. The transition corresponds to an order–disorder transition from a homogeneous solution to a microphase separated structure consisting of highly swollen lamellae. There are, however, essential differences between the two classes of systems. In the case of physical association the amount of polar and nonpolar material is comparable. The polymacromonomers, on the other hand, contain only an extremely small fraction of backbone material, of the order of 1 to 2 wt %. So, the structures can in a good approximation be considered as consisting of pure polystyrene only, with a very dense almost globular core and a much less dense corona. In this case a block copolymer like order–disorder transition should not be expected. In fact, the good solvent introduces an effective repulsion between the coronas of these polymacromonomers. As a consequence a characteristic length of the order of the size of the diameter is present in these solutions. The individual bottle-brush structures, based on the dynamic light scattering data, have an internal density of ~ 0.26 g/mol. This estimation is based on $D \cong 100$ Å, $\lambda \cong 1400$ Å, and $M_w \cong 2.2 \times 10^6$ g/mol.[1] Hence, these bottle-brushes do not overlap until polymer concentrations in the order of 30 wt % are reached, a number that happens to coincide with the concentration for which a sharp small angle x-ray scattering peak was observed for the first time. At the critical overlap concentration the *intermolecular* bottle-brush repulsion apparently results in a sharp Bragg reflection. However, the relation with the conventional nematic transition in semiflexible polymer solutions, such as aromatic polyamides solutions, is less obvious.

Because the situation is rather unclear, we decided to investigate molecular bottle-brushes in a dilute good solvent by continuous space Monte Carlo computer simulations, the results of which will be reported in this paper. A few related systems[23–26] have been published in recent years and in particular, the bond fluctuation lattice model study by Rouault and Borisov[23] deserves mentioning. Our simulations address structures with an effectively higher coverage and a much stronger excluded volume effect between successive side chains, which is the essential parameter with respect to lyotropic behavior.

II. THEORETICAL APPROACH

Before we discuss the computer simulation methodology and present the results, it is useful to consider briefly the theoretical approaches that have been published so far. The most extensive study is due to Fredrickson[22] who considered bottle-brushes obtained by association between homopolymers and end-functionalized oligomers. Here we are not interested in the chemical equilibrium that is involved and discuss the properties of the bottle-brush structures assuming the side chains are securely fixed. His starting point is the free energy of a comb copolymer structure in the limit of low coverage with side chains, which as a straightforward generalization of Flory's approach,[27,28] is given by

$$\beta F = \frac{R^2}{Na^2} + a^3 \frac{N^2}{R^3} + R_M^3 \frac{(\sigma N)^2}{R^3}, \tag{1}$$

here R is the size of the main chain of N beads of size a^3, σN is the number of side chains of M beads of size a^3 each, R_M denotes the Flory radius of the side chains and $\beta = 1/kT$. On the basis of this expression three different regimes can be distinguished:

(a) **Low coverage: $\boldsymbol{\sigma \ll M^{-9/10}}$**. Here, the successive side chains are on average so far away from each other that the beads of the polymer backbone determine the excluded volume and, hence the result is the familiar Flory expression $R \cong aN^{3/5}$.

(b) **Low to intermediate coverage: $\boldsymbol{M^{-9/10} \ll \sigma \ll M^{-3/5}}$**. Here the excluded volume is determined by the side chains and the size of the structure is the result of the balance between the unfavorable elastic stretching of the main chain and the corresponding reduction in excluded volume from the side chains: $R \cong a\sigma^{2/5} M^{9/25} N^{3/5}$.

(c) **High coverage: $\boldsymbol{\sigma \gg M^{-3/5}}$**. In this regime the side chains begin to overlap severely and the free energy Eq. (1) ceases to be valid. An extended rodlike state for the polymer backbone is predicted together with side chains that behave essentially like two-dimensional self-avoiding walks in a plane perpendicular to the spine, i.e., $R_M \cong aM^{3/4}$. A sta-

bility analysis of this extended conformation led Fredrickson to the conclusion that the persistence length satisfies $\lambda \sim a\sigma^{17/8}M^{15/8}$. Because R_M is proportional to the diameter D of the bottle-brush structure, the last two equations demonstrate that $\lambda/D \sim M^{9/8}$. Since this ratio increases monotonously with the side chain length, lyotropic behavior should be the rule.

Birshtein *et al.*[19] took a somewhat different approach writing the free energy of the bottle-brush as a sum of two terms

$$\beta F = \Delta F_{\mathrm{el}}(\sigma^{-1},h) + \Delta F(M,h). \tag{2}$$

The second term represents the free energy of chains of length M attached to a solid cylinder with a distance h between successive side chains. The first term represents the elastic free energy of stretching a self-avoiding walk of σ^{-1} segments (i.e., the number of segments between two successive side chains in the bottle-brush model introduced in the above discussing dealing with Fredrickson's approach) up to length h. For large extensions this term can be found in De Gennes,[27] Eq. I.49

$$\Delta F_{\mathrm{el}} \cong (h\sigma^{3/5})^{5/2}. \tag{3}$$

For the second term they derived an expression, which was later also given by Wang and Safran[29]

$$\Delta F \cong h^{-5/8}M^{3/8} \tag{4}$$

Minimizing Eq. (2) with respect to h then gives the equilibrium value of h and this in turn determines the local structure, using the concepts on which Eq. (2) is based. In this way they obtained for the overall size of the structure $R \cong a\sigma^{9/25}M^{9/25}N^{3/5}$, which happens to be nearly identical to the expression obtained by Fredrickson in the low to intermediate covering regime. For the diameter they find

$$D \cong a\sigma^{3/25}M^{18/25} \sim M^{0.72}, \tag{5}$$

with an exponent which is slightly smaller than the 2D-SAW value of 3/4 due to the assumption that a chain section between two successive side chains can be stretched beyond any limit. If this is no longer the case, we automatically enter the extended cylinder regime where the exponent will be 3/4.[19,29] Therefore, we conclude that the above analysis indeed addresses the intermediate coverage limit. As far as the possibility of lyotropic behavior is concerned, the authors[19] speculate that the persistence length of the bottle-brush structure will be of the same order of magnitude as its diameter and hence, that lyotropic behavior due to excluded volume effects alone should not be expected. Here, their opinion obviously differs with that of Fredrickson, who on the basis of an analysis of a fully stretched structure came to the exact opposite conclusion.

In a very recent paper, Rouault and Borisov[23] also discussed comb copolymers. Using a Flory approach which differs slightly from Eq. (1), they find $R \cong a\sigma^{0.4}M^{0.4}N^{3/5}$. Under conditions of dense grafting of long side chains where a simple Flory argument breaks down, they find $R \cong a\sigma^{0.54}M^{0.54}N^{3/5}$. Although stiffening of the backbone is an important ingredient, the possibility of lyotropic behavior is not discussed in any detail.

Since these treatments involve scaling arguments it is very difficult to assess the consequences for real polymer systems. If very long side chains are required, then a serious question arises concerning the polymer concentration for which lyotropic behavior may be expected. Suppose that for a certain value of M ($N \gg M$), the ratio between the persistence length λ and the diameter D is indeed sufficiently large ($\lambda/D > 10$), then the density of polymer segments ρ in a single bottle-brush satisfies

$$\rho \cong \frac{\lambda(\sigma M+1)}{\lambda D^2 a} \sim M^{-1/2}, \tag{6}$$

where use has been made of $D \sim M^{3/4}$. This simply implies that bottle-brushes will start to overlap at rather low concentrations for M large. Since the very idea of lyotropic behavior of bottle-brushes is based on the role of the excluded volume effect, which will gradually diminish above the overlap concentration, nematic behavior of molecular bottle-brushes will have to disappear again at somewhat higher polymer concentrations.

III. MODEL AND DETAILS OF THE SIMULATION

Monte Carlo (MC) simulations were used to study the conformational properties of bottle-brush copolymers. The copolymers were modeled in 3D continuous space as linear chains of hard spheres freely jointed together, to which side chains consisting of hard spheres of the same size are grafted. The distance between the centers of mass of successive beads is arbitrarily set to one and the radius of the beads in the same units equals 0.5. Since the whole issue of lyotropic behavior of bottle-brushes is intimately connected with the excluded volume effect between nonbonded beads, the only interactions in the system will be hard-sphere interactions and the potential energy takes the simple form

$$U_{ij} = \begin{cases} 0 & \text{if } i \text{ and } j \text{ are neighbors or } r_{ij} > 1, \\ \infty & \text{otherwise} \end{cases}, \tag{7}$$

where r_{ij} is the distance between beads i and j. Solvent interactions are explicitly ignored in this approach, and the model corresponds to a bottle-brush in an athermal solution.

Configuration space is sampled according to the Metropolis importance sampling scheme.[30] For every trial step it is first decided whether an attempt to move a main chain bead or a side chain bead is taken according to a predescribed probability. After that a bead is chosen randomly from the main chain beads or from all the side chain beads. A small chain requires considerably less steps to equilibrate than a large one. In fact the relaxation time τ for a chain of N beads in a good solvent in the case of free draining is known to scale like $\tau \sim N^{11/5}$, whereas $\tau \sim N^2$ for the Rouse model. Since both exponents are close to two, the choice to attempt to move a main chain bead or a side chain bead is made according to the relaxation time being proportional to N^2. Let the number of main chain beads be denoted by N,

the number of beads per side chain by M and the total number of side chains n_s, then the probability of taking a main chain bead p is given by

$$p = \frac{N^3}{n_s M^3 + N^3}. \tag{8}$$

Here the number of beads appears with the power 3, since every bead must have the opportunity to move once to define a elemental time step, which introduces another factor N for main chain beads and M for side chain beads.

To introduce the trial moves, three different kinds of beads have to be distinguished:

(a) **''Common bead'':** This is every bead that is neither a chain end bead nor a main chain bead connected to a side chain; the trial move consists of a rotation over a randomly chosen angle around the vector connecting its neighboring beads.

(b) **''Grafted main chain bead'':** Here the trial move is the same as above, except that the side chain connected to it is also rotated in a concerted manner.

(c) **''Chain end bead'':** The trial move consists again of a rotation over an arbitrary angle, however, this time around the vector connecting beads $N-1$ and $N-3$, taking bead N to be the chain end bead. This allows the bond angles to change also at the ends of the chain.

Figure 1 illustrates the three different possibilities. The acceptance of the trial move is easy to determine, since the potential-energy change at every step is either zero (accepted) or infinite (rejected).

The studied structures consisted of 100 main chain beads (99 chain segments) with 50 side chains of M beads each. The main chain beads from which a side chain is grafted were chosen equally along the backbone, i.e., every other main chain bead carried a side chain. Side chains of lengths $M = 0$, 4, 6, 8, 10, 12, 16, and 20 were considered. The initial conformation was created in the following way. First the backbone was formed as a hard-sphere self-avoiding walk in the first quadrant of a two-dimensional plane. Then the side chains were grown from this backbone randomly in three-dimensional space. Every bottle-brush structure was equilibrated by running the simulation for $5*10^5$ Monte Carlo (MC) main chain steps and $50*M^2$ MC side chain steps. Here a MC step refers to some elemental time and thus differs between the main chain and the side chain. For the main chain it corresponds to 100 ($= N$) attempts and for the side chains to $50*M$ attempts. After equilibration the simulation was divided into 10 blocks, each consisting of $100*N^2$ MC main chain steps ($= 10^6$ MC steps) and $100*M^2$ MC side chain steps. For every block the average values of the quantities of interest were calculated using 500 conformations taken from the simulation at equally spaced intervals. The average of the block averages $\langle A\rangle_{\text{block}}$ was then used as an estimate for the average quantity $\langle A\rangle$. The statistical errors were calculated assuming that each block average value is an independent sample from a Gaussian distribution with unknown variance. In that case, using numerical values of the Student-t distribution with nine degrees of freedom, we obtain for 95% confidence interval:

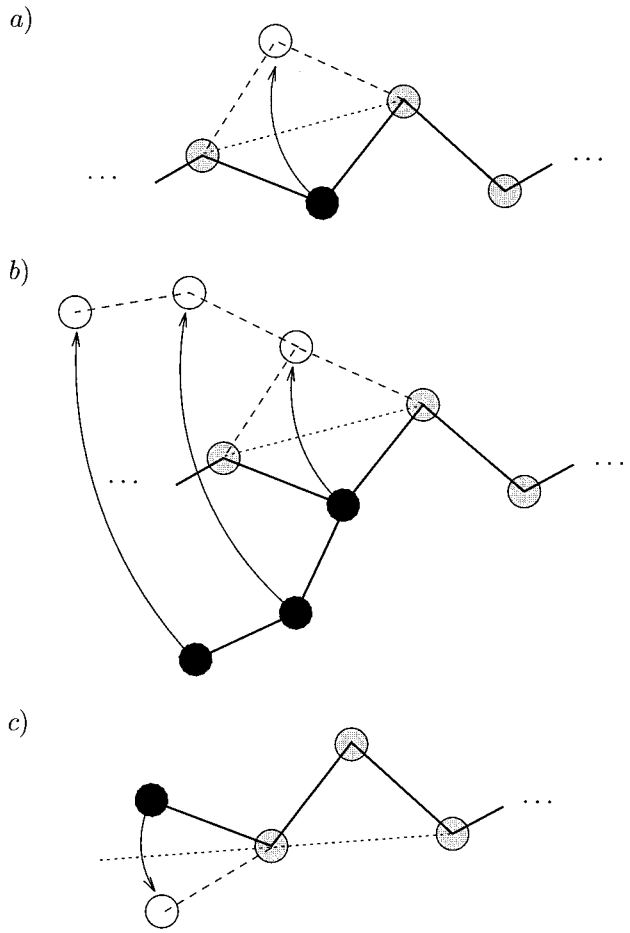

FIG. 1. Illustration of the Monte Carlo moves. (a) Bead that is neither an end bead, nor a main chain bead connected to a side chain; (b) Main chain bead connected to a side chain; (c) End bead.

$$\langle A\rangle = \langle A\rangle_{\text{block}} \pm 0.72\sigma(\langle A\rangle_{\text{block}}), \tag{9}$$

where $\sigma(\langle A\rangle_{\text{block}})$ is the standard deviation of the block averages.

IV. RESULTS

In this section we will present the results of our Monte Carlo simulations on a bottle-brush consisting of a main chain of 100 beads and 50 side chains of 0–20 beads. Occasionally, we will refer to some smaller structures of main chains of 50 beads with a complete coverage, i.e., also with 50 side chains. In the latter case chain end effects are more important and to minimize these only the middle part will be considered. For the main chain of 100 beads end effects are less important, but will be considered where necessary. The possibility of lyotropic behavior of molecular bottle brushes depends directly on the ratio between the persistence length and the diameter, so this will be our primary concern. Then the polymer backbone will be characterized in terms of the radius of gyration tensor and asphericity and finally the whole structure will be characterized in the same way. Figure

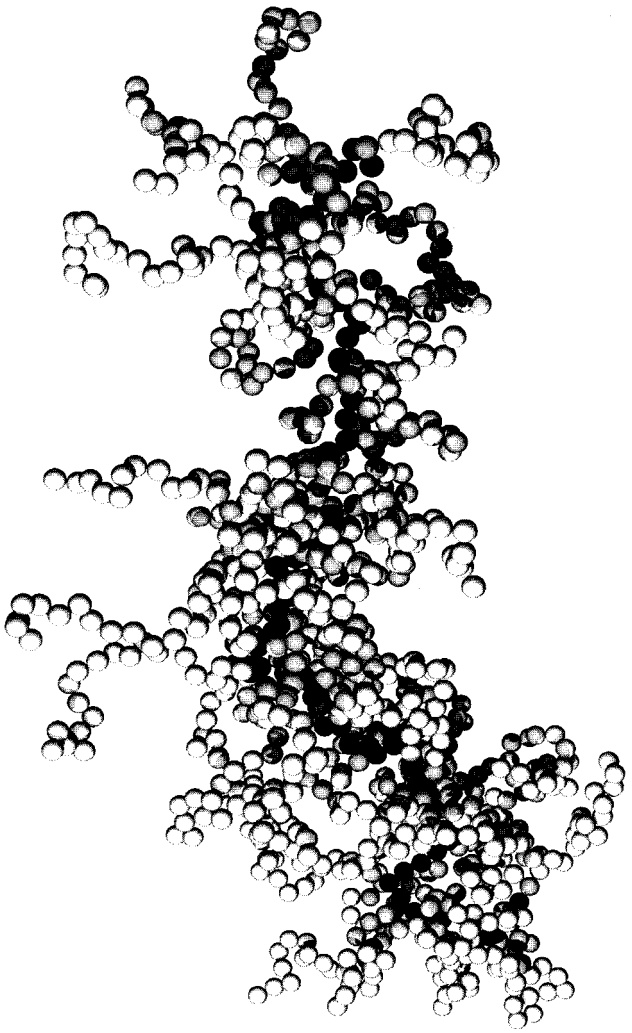

FIG. 2. Characteristic bottle-brush conformation of a main chain (black) of 100 beads and 50 side chains (white) of 20 beads each.

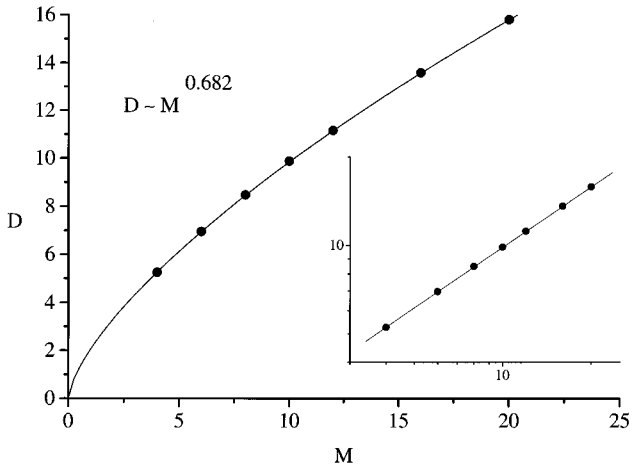

FIG. 3. The diameter D of the bottle-brush structure as a function of side chain length M.

2 shows a characteristic conformation of the largest bottle-brush structure simulated. It illustrates many of the features that will be discussed and we will refer to it time and again.

A. Persistence length and bottle-brush diameter

The first problem to deal with is how to define these quantities. From the theoretical section the definition of the diameter D as twice the root-mean-square average of the end-to-end distance of the side chains is the obvious choice and this is where we start. Figure 3 shows D as a function of M. Since the data are obtained by averaging over the end-to-end distance of all side chains, the error bars are even smaller than the symbols used to present the data. Furthermore, leaving a certain number (10 or even more) of side chains situated at either end of the main chain out makes no difference. As is also clear, the fitting of the monotonously increasing function is almost perfect and leads to a scaling prediction $D \sim M^{0.682}$. The same exponent follows from the log–log plot presented as an inset in the same figure. This value of the exponent is still smaller than the 0.72 derived by Birshtein and co-workers[19] and the 0.75 given by Fredrickson,[22] however, it is at the same time much larger than the 3D SAW value of 0.588. So, although we are obviously far away from the real scaling regime, it is quite obvious that the excluded volume effect is operational for our structures. Rouault and Borisov,[23] on the other hand, still find the ''unperturbed'' 3D-scaling $M^{0.6}$ for the size of the side chains of the structures they study and comment, that it is not surprising because the degree of overlap is still rather weak.

For the persistence length things are not so clear. Since, the backbone is supposed to become extended rodlike at high coverages, we decided to use expressions pertaining to the wormlike chain model. However, it should be realized that this model interpolates between a rodlike and a *random* walk structure. In other words, excluded volume effects due to the self-avoiding character of the backbone conformation are not included. We start with the familiar relation between the persistence length λ and either the end-to-end distance R_e or the radius of gyration R_g, since this is the preferred method used to interpret experimental results. Of course, there is a subtle difference, experimentally it is applied to the whole structure, whereas we apply it to the backbone only. After that an alternative analysis based on the bond angle correlation function will be presented. The first mentioned equations are[31]

$$R_e^2 = \langle R^2 \rangle = 2L\lambda - 2\lambda^2(1 - e^{-L/\lambda}), \tag{10}$$

$$R_g^2 = \langle S^2 \rangle = \frac{L\lambda}{3} - \lambda^2 + \frac{2\lambda^3}{L} - \frac{2\lambda^4}{L^2}(1 - e^{-L/\lambda}), \tag{11}$$

where $L = Na = N$, and R and S represent the end-to-end distance and the radius of gyration of a particular conformation. It was this latter equation which was used by Schmidt and co-workers[1,2] to calculate the persistence length of the polymacromonomers from dilute solution scattering measurements. The results required are therefore the end-to-end distance and the radius of gyration of the backbone as a function of the side chain length M. Since both lead to essentially the same predictions, we restrict ourselves to the radius of gyration. The data are presented in Fig. 4 and show

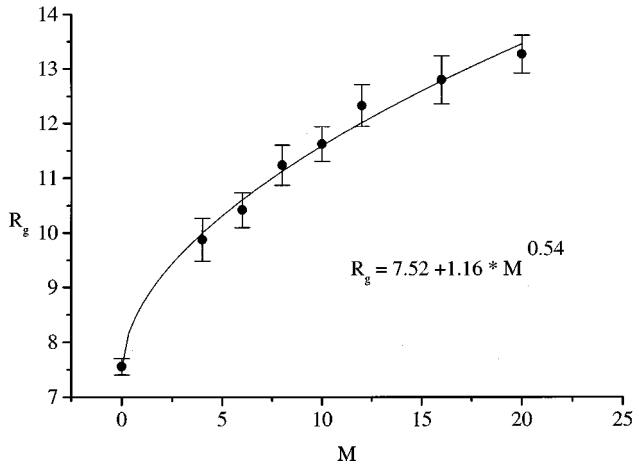

FIG. 4. Radius of gyration R_g of the main chain as a function of side chain length M.

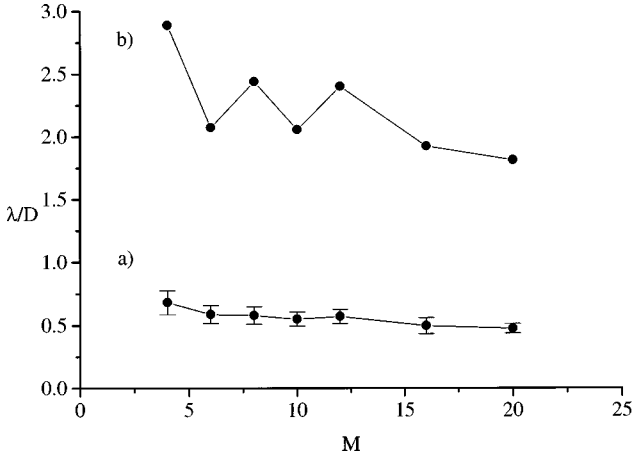

FIG. 6. (a) The ratio of persistence length λ, based on Eq. (11), and the diameter D as a function of M. (b) The ratio of the persistence length λ, obtained from the correlation data of Fig. 7, and the diameter D.

R_g to increase monotonously with M giving the first indication of side chain induced stretching. The data have been fitted with a power law equation which indicates an increase with an exponent close to 0.54. In this case, a log–log plot is not suitable because of the important contribution of the constant corresponding to $M = 0$. Only for very large values of M would this be possible. In the theoretical section various exponents were given. Perhaps fortuitously, our exponent agrees surprisingly well with the exponent 0.54 theoretically predicted by Rouault and Borisov[23] for the situation of dense grafting with long side chains.

Figure 5 presents the persistence length as a function of M as obtained from the radius of gyration. Although not shown, using the end-to-end distance leads to nearly identical results, as it should of course. The data show also a monotonously increasing behavior, which using similar fitting as before now leads to a scaling of $\lambda \sim M^{0.7}$, a result that is not even close to the predictions of Fredrickson[22] of $\lambda \sim M^{1.875}$. Before this is discussed any further, the ratio between the persistence length and the diameter as it follows from these results will be considered. The data are presented in Fig. 6(a) and demonstrate a most striking behavior. Rather than increasing as a function of M, the best one can say is that the slight decrease of this ratio levels off. However, before jumping to any conclusion, the possibility of more than one characteristic length scale should be considered. Already the conformation presented in Fig. 2 illustrates that the backbone is rather flexible at small length scales and becomes extended on a larger length scale only. As a consequence, the calculations presented underestimate the value of the persistence length that we are really interested in. In order to investigate this issue, the bond angle correlation function, defined as the average cosine $\langle \cos \theta(s) \rangle$ of the angle between chain segments separated by a length s was calculated. The relation between the bond correlation function and the persistence length λ of a persistent chain is given by

$$\langle \cos\ \theta(s) \rangle = e^{-s/\lambda}. \tag{12}$$

Selected results ($M = 0,6,10,16,20$) are presented in Fig. 7. The large scatter in data for increasing values of s results

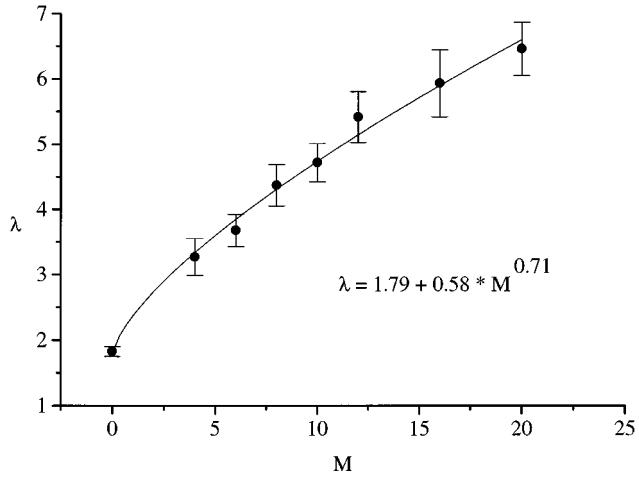

FIG. 5. Persistence length λ of the main chain based on R_g as a function of side chain length M.

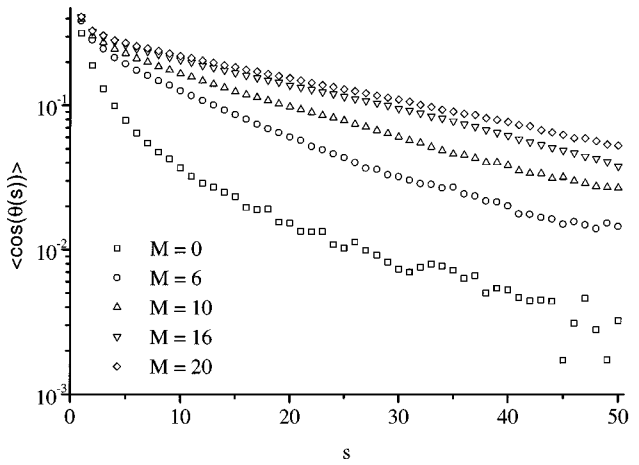

FIG. 7. Bond correlation $\langle \cos \theta(s) \rangle$ as a function of s for $M = 0$, 6, 10, 16, and 20.

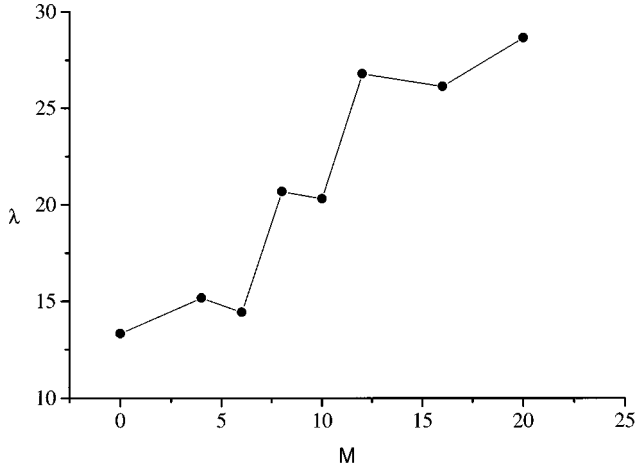

FIG. 8. Persistence length λ of the main chain obtained by applying Eq. (12) to the correlation data presented in Fig. 7, as a function of side chain length M.

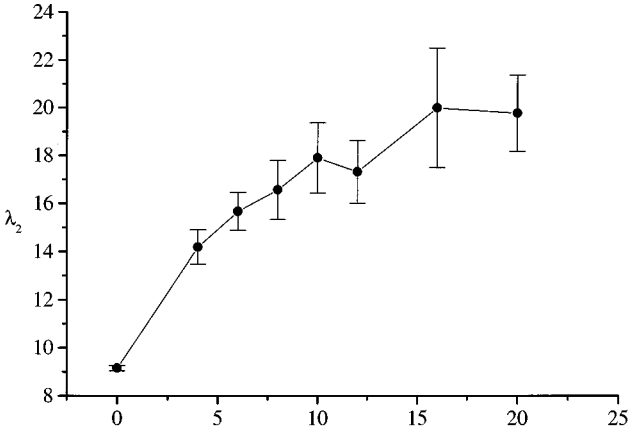

FIG. 10. The middle eigenvalue λ_2 of the main chain as a function of M.

from the decreasing number of data points involved. Several observations can be made. First, the excluded volume effect between the backbone beads, manifestly present for small values of M, introduces an effective persistence to the chains. This effect is most obvious for $M = 0$, but continues to play a role for higher values of M. Furthermore, all curves show a strong decline for small values of s, which represents the local small length scale flexibility of the backbone. It is this fact that results in an underestimation of the persistence length using the $R_g(\lambda)$ expression Eq. (11). The most appropriate procedure is to use the middle linear part of the curves. This type of fitting leads to values of the persistence lengths presented in Fig. 8. The values are considerably larger than the ones calculated on the basis of Eqs. (10) and (11). Due to the excluded volume effect, the new data present an upper bound. Because of the arbitrariness involved, except maybe for the largest values of M, error bars have been omitted. The fact that the excluded volume effect diminishes for more extended conformations, lends some credibility to these values, in particular to the ones obtained for the larger values of M. These results indicate that, at least for M not too small, it is possible to characterize the structure rather well in terms of a persistent structure. The ratio between λ obtained in this way and the diameter D is also presented in Fig. 6(b). Although it is considerably larger now, the qualitative behavior as a function of M is the same as before.

So, that leaves us with the following tentative conclusions. From the data for the diameter it is clear that the longer side chains are long enough to induce considerable stretching of both the side chains and the main chain. This confirms that the structures with the longer side chains are at least in the ''intermediate covering regime.'' The fact that no clear increase in the ratio between the persistence length and diameter for increasing values of M is found leaves essentially two possibilities open. Either, we are still too far away from the strong stretching regime, or, which seems more likely, our results support the conclusion by Birshtein and co-workers[9] that this ratio becomes independent of the side chain length. Additional support for this conclusion comes from the observation of Rouault and Borisov[23] that the fluctuations in the main chain configuration may result in a significant decrease in the induced backbone extension, fluctuations that were not taken into account in the Fredrickson approach.[22] These conclusions do not exclude lyotropic behavior; it is still possible that the excluded volume interaction between different bottle-brushes induces additional stretching.

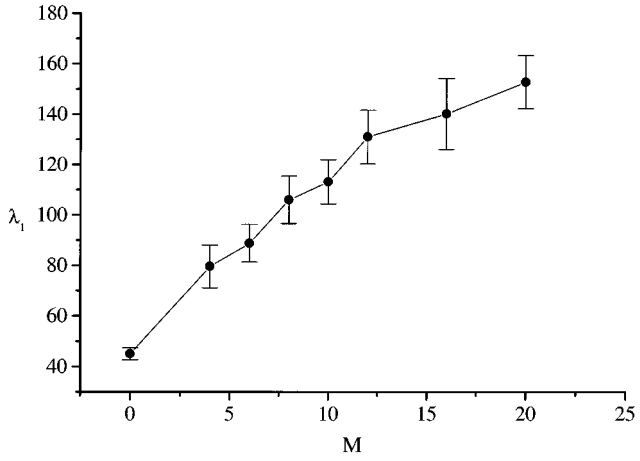

FIG. 9. The largest eigenvalue λ_1 of the main chain as a function of M.

B. Characterization of backbone and bottle-brush structure

In the final section we will characterize the backbone and the bottle-brush structure in a little more detail. This characterization can best be done[32] by means of the radius of gyration tensor T defined by

$$T_{\alpha\beta}=\frac{1}{N}\sum_{i=1}^{N}(r_{i,\alpha}-r_{\text{c.m.},\alpha})(r_{i,\beta}-r_{\text{c.m.},\beta}), \tag{13}$$

where α and β refer to the x, y, and z components of the position of the main chain beads ($r_{i,\alpha}$) and the center of mass of the main chain ($r_{\text{c.m.},\alpha}$). Hence the elements of the matrix are products of the x, y, and z components of the

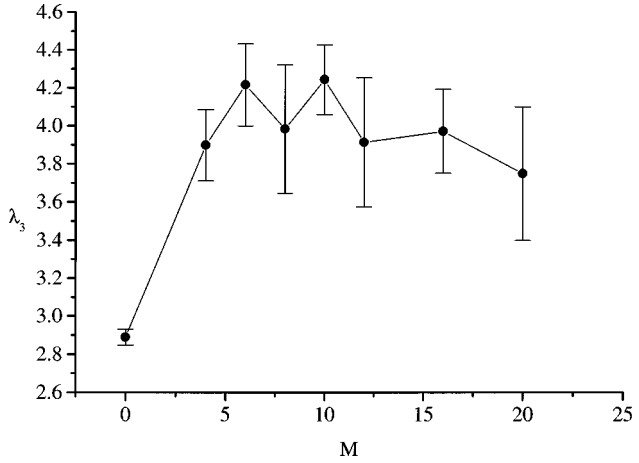

FIG. 11. The smallest eigenvalue λ_3 of the main chain as a function of M.

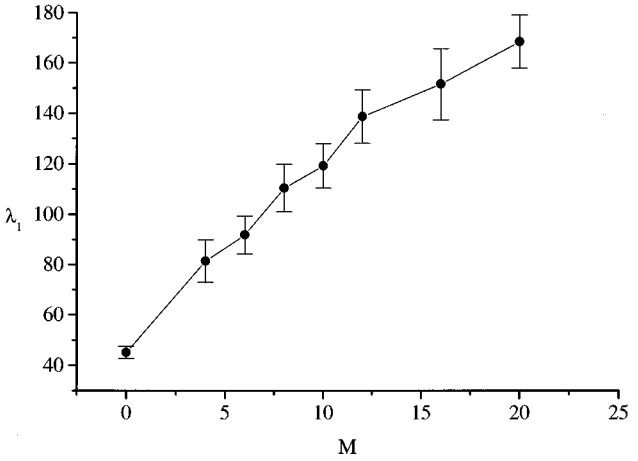

FIG. 13. The largest eigenvalue λ_1 of the bottle-brush structure as a function of M.

radius of gyration. The radius of gyration tensor was first introduced by Solc and Stockmayer[33] in their study of random flight chains. The eigenvalues of T, in descending order denoted by λ_1, λ_2, and λ_3, are called the principal radii of gyration. They are related to the radius of gyration by

$$R_g^2=\lambda_1+\lambda_2+\lambda_3. \tag{14}$$

These eigenvalues may be considered as the square lengths of the principal axes of an ellipsoid describing the shape of the structure. The corresponding eigenvectors define the direction of the principal axes, the largest eigenvalue corresponding to the preferred direction of the object.

Figures 9–11 present the principal radii of gyration of the main chain backbone as a function of side chain length M. Comparing the M dependence of the three eigenvalues, we note that the largest one, λ_1, not unexpectedly shows the strongest increase. The middle one, λ_2, also increases but not as strongly. The most interesting observation, however, is the slight decrease in the smallest eigenvalue λ_3. Apparently, this is the way the stretching manifests itself in terms of the principal radii of gyration. Another measure of the shape of an object is given by the quantity A_d called asphericity. Mathematically it is defined by

$$A_d=\frac{\Sigma_{i>j}\langle(\lambda_i-\lambda_j)^2\rangle}{2\langle(\Sigma_{i=1}^{3}\lambda_i)^2\rangle}, \tag{15}$$

and it has zero as a lower bound for a spherical object. In the case of Random Walks it can be calculated exactly in any dimension,[32] being $10/19 \cong 0.53$ in 3D. For self-avoiding walks the value in 3D is slightly larger, ~ 0.54. Figure 12 represents A_d as a function of side chain length M for the main chain backbone. A steadily increase is observed, indicating a shape that deviates more and more from spherical.

Having so far concentrated on the polymer backbone, next we will consider the complete structure. Figures 13–15 present the data for λ_1, λ_2, and λ_3. Now, there are clear differences with the previous results describing only the backbone. In particularly, the strong increase in the smallest eigenvalue λ_3 should be noted. This is of course due to the side chains, but the most striking observation arises from the behavior of the ratio λ_2/λ_3, presented in Fig. 16. This ratio is falling down rapidly as a function of M, a clear indication for a more cylindrically like shape of the bottle-brush. The asphericity of the bottle brush, presented in Fig. 17, behaves

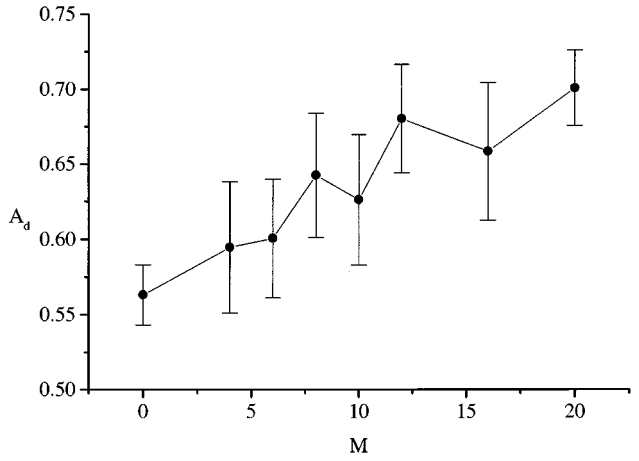

FIG. 12. Asphericity A_d of main chain as a function of M.

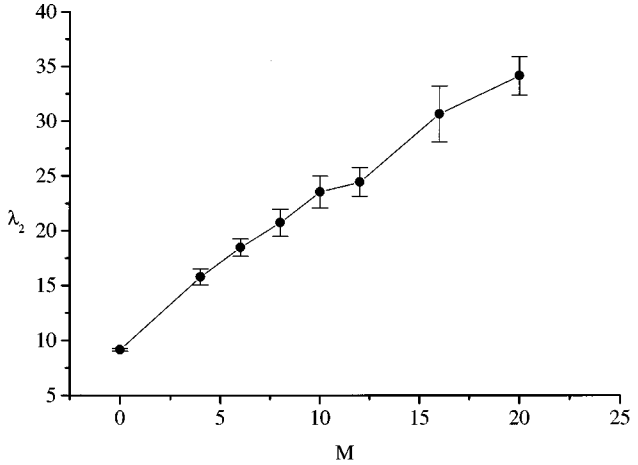

FIG. 14. The middle eigenvalue λ_2 of the bottle-brush structure as a function of M.

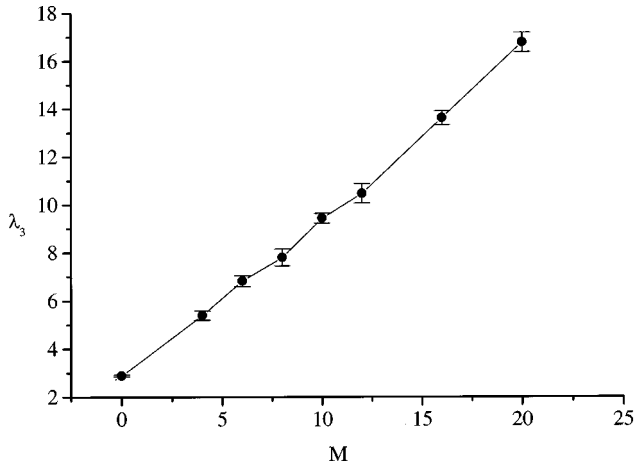

FIG. 15. The smallest eigenvalue λ_3 of the bottle-brush structure as a function of M.

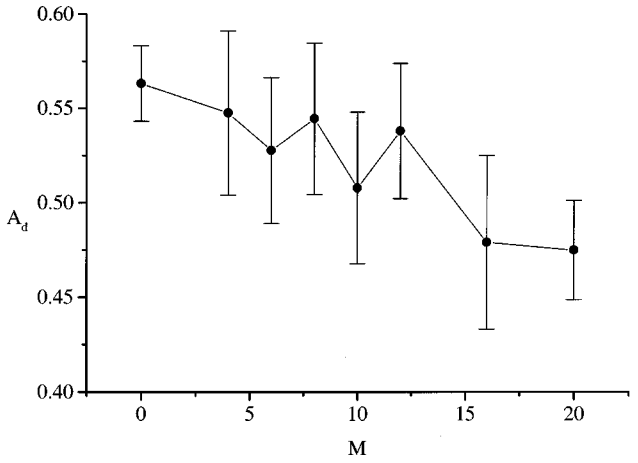

FIG. 17. Asphericity A_d of the bottle-brush structure as a function of M.

completely opposite from that of the backbone. It decreases as a function of M, which could be interpreted as the structure becoming more spherical. This seems counter intuitive, however, it should not really come as a surprise because the increase in length of the side chains is felt strongest by the smallest component. Because N is kept constant the structure becomes, despite the stretching more spherical for increasing M.

V. CONCLUDING REMARKS

The 3D continuous space Monte Carlo simulations presented concern freely jointed hard-sphere chains grafted with freely jointed hard-sphere side chains. The beads of the main chain and of the side chain have identical size. Even for the largest structure studied, consisting of 100 main chain beads and 50 side chains of 20 beads each, the extension of the backbone is such that the value of the persistence length is less than twice the value of the diameter. This finding shows that lyotropic behavior of these kind of bottle-brushes, based exclusively on the side chain induced extension is highly unlike solely increasing the length of the side chains. Since not even a beginning of an upturn in the behavior of the ratio between persistence length and diameter is observed, it is not so unreasonable to speculate that if sufficient stretching can be induced, the side chains have to be at least 1 or 2 orders of magnitude larger; well beyond present day computer simulation possibilities. This implies also that, using Eq. (6), the segment density inside a single bottle-brush will then be of the order of a few percents at most. Consequently, overlap between bottle-brushes will occur already at rather low concentrations. In the semidilute regime, the molecules may at first stretch more, but ultimately the excluded volume effect, on which the very extension is based, will be screened. Then the nematic behavior of individual bottle-brushes will also disappear.

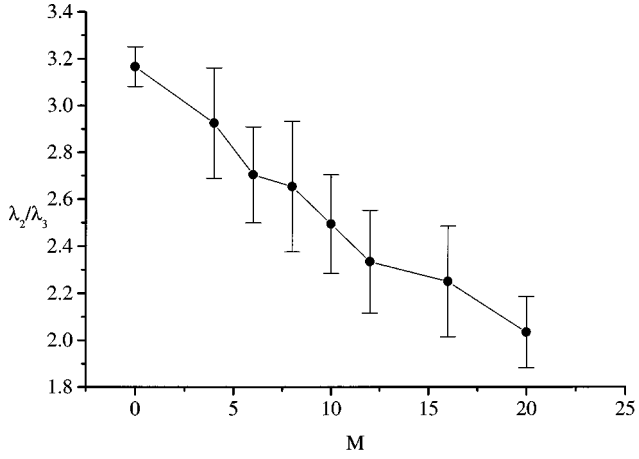

FIG. 16. The ratio λ_2/λ_3 for the bottle-brush structure as a function of M.

The final question remains, how to interpret some of the existing experimental data. First of all, it should be realised that the beads of our model are of equal size for the main chain and the side chain. In the experimental example cited before, due to Schmidt and co-workers,[1,2] the main chain was polymethacrylate and the side chains were polystyrenes. However, the size of the styrene monomers is undoubtedly bigger than the size of the methacrylate monomers. Moreover, both the main chain and the side chains are considerably stiffer than a freely jointed chain. They may be treated as a freely jointed chain of flexible segments, only these flexible units would comprise several monomers. In terms of Kuhn segments the length of the polystyrene side chains are essentially comparable to the longer side chains we used. Concentrating on the main chain, this implies that there are actually several side chains per flexible main chain segment. These two effects, a considerably higher coverage (at least effectively), as well as a larger excluded volume per side chain bead than per main chain bead, might explain the extremely large persistence length observed. This suggests to study whether lyotropic behavior can be induced by adjusting the topology of the side chains, instead of increasing their length. In fact, the preliminary computer simulations suggest that the size of the side chains has an important role to control the extension.[34]

ACKNOWLEDGMENTS

The work has been supported by Finnish Academy, Technology Development Centre (Finland) and Neste Foundation. Risto Nieminen/CSC Finland is acknowledged for providing computing time. At Purdue this work is supported by NSF grant CTS-9624268.

[1] M. Wintermantel, K. Fischer, M. Gerle, R. Ries, M. Schmidt, K. Kajiwara, H. Urakawa, and I. Wataoka, Angew. Chem. **107**, 1606 (1995).
[2] M. Wintermantel, M. Gerle, K. Fischer, M. Schmidt, I. Wataoka, H. Urakawa, K. Kajiwara, and Y. Tsukahara, Macromolecules **29**, 978 (1996).
[3] M. Antonietti, J. Conrad, and A. Thünemann, Macromolecules **27**, 6007 (1994).
[4] M. Antonietti and J. Conrad, Angew. Chem. Int. Ed. Engl. **33**, 1869 (1994).
[5] M. Antonietti, C. Burger, and J. Effing, Adv. Mat. **7**, 751 (1995).
[6] M. Antonietti and M. Maskos, Makromol. Rapid Commun. **16**, 763 (1995).
[7] M. Antonietti, A. Wenzel, and A. Thünemann, Langmuir **12**, 2111 (1996).
[8] J. Ruokolainen, G. ten Brinke, O. Ikkala, M. Torkkeli, and R. Serimaa, Macromolecules **29**, 3409 (1996).
[9] J. Ruokolainen, M. Torkkeli, R. Serimaa, E. Komanschek, O. Ikkala, and G. ten Brinke, Phys. Rev. E **54**, 6646 (1996).
[10] J. Ruokolainen, M. Torkkeli, R. Serimaa, S. Vahvaselkä, M. Saariaho, G. ten Brinke, and O. Ikkala, Macromolecules **29**, 6621 (1996).
[11] J. Ruokolainen, M. Torkkeli, R. Serimaa, B. E. Komanschek, G. ten Brinke, and O. Ikkala, Macromolecules **30**, 2002 (1997).
[12] O. Ikkala, J. Ruokolainen, G. ten Brinke, M. Torkkeli, and R. Serimaa, Macromolecules **28**, 7088 (1995).
[13] H. Benoit and G. Hadziioannou, Macromolecules **21**, 1449 (1988).
[14] A. V. Dobrynin and I. Y. Erukhimovich, Macromolecules **26**, 276 (1993).
[15] D. P. Foster, D. Jasnow and A. C. Balazs, Macromolecules **28**, 3450 (1995).
[16] A. Shinozaki, D. Jasnow, and A. C. Balazs, Macromolecules **27**, 2496 (1994).
[17] F. Tanaka, Advances in Colloid and Interface Science **63**, 23 (1996).
[18] F. Tanaka and M. Ishida, Macromolecules **30**, 1836 (1997).
[19] T. M. Birshtein, O. V. Borisov, Y. B. Zhulina, A. R. Khokhlov, and T. A. Yurasova, Polym. Sci. USSR **29**, 1293 (1987).
[20] L. Onsager, Ann. N.Y. Acad. Sci. **51**, 627 (1949).
[21] A. Khokhlov and A. N. Semenov, Physica A **108**, 546 (1981).
[22] G. H. Fredrickson, Macromolecules **26**, 2825 (1993).
[23] Y. Rouault and O. V. Borisov, Macromolecules **29**, 2605 (1996).
[24] L. V. Gallacher and S. Windmer, J. Chem. Phys. **44**, 1139 (1966).
[25] F. L. McCrackin and J. Mazur, Macromolecules **14**, 1214 (1981).
[26] J. E. G. Lipson, Macromolecules **24**, 1327 (1991).
[27] P.-G. de Gennes, *Scaling Concepts in Polymer Physics* (Cornell University Press, Ithaca, New York, 1979).
[28] P. J. Flory, *Principles of Polymer Chemistry* (Cornell University Press, Ithaca, New York, 1971).
[29] Z.-G. Wang and S. A. Safran, J. Chem. Phys. **89**, 5323 (1988).
[30] N. Metropolis, A. W. Rosenbluth, M. N. Rosenbluth, A. H. Teller, and E. Teller, J. Chem. Phys. **21**, 1087 (1953).
[31] H. Yamakawa, *Modern Theory of Polymer Solutions* (Harper & Row, New York, 1971).
[32] J. Rudnic and G. Gaspari, Science **237**, 384 (1987).
[33] K. Solc and W. H. Stockmayer, J. Chem. Phys. **54**, 2756 (1971).
[34] M. Saariaho, I. Szleifer, O. Ikkala, and G. ten Brinke (unpublished).